Accepted Manuscript

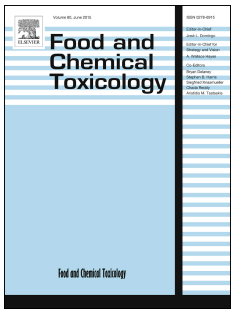

Toxicological assessment of silica-coated iron oxide nanoparticles in human astrocytes

Natalia Fernández-Bertólez, Carla Costa, Fátima Brandão, Gözde Kiliç, José Alberto Duarte, Joao Paulo Teixeira, Eduardo Pásaro, Vanessa Valdiglesias, Blanca Laffon

PII: S0278-6915(18)30281-3

DOI: 10.1016/j.fct.2018.04.058

Reference: FCT 9747

To appear in: *Food and Chemical Toxicology*

Received Date: 2 February 2018

Revised Date: 23 April 2018

Accepted Date: 25 April 2018

Please cite this article as: Fernández-Bertólez, N., Costa, C., Brandão, Fá., Kiliç, Gö., Duarte, José.Alberto., Teixeira, J.P., Pásaro, E., Valdiglesias, V., Laffon, B., Toxicological assessment of silica-coated iron oxide nanoparticles in human astrocytes, *Food and Chemical Toxicology* (2018), doi: 10.1016/j.fct.2018.04.058.

Toxicological assessment of silica-coated iron oxide nanoparticles in human astrocytes

Natalia Fernández-Bertólez[a,b], Carla Costa[c,d], Fátima Brandão[c,d], Gözde Kiliç[a], José Alberto Duarte[e], Joao Paulo Teixeira[c,d], Eduardo Pásaro[a], Vanessa Valdiglesias[a,d,*,†] Blanca Laffon[a,†]

[a]*Universidade da Coruña, DICOMOSA Group, Department of Psychology, Area of Psychobiology, Edificio de Servicios Centrales de Investigación, Campus Elviña s/n, 15071-A Coruña, Spain*

[b]*Universidade da Coruña, Department of Cell and Molecular Biology, Facultad de Ciencias, Campus A Zapateira s/n, 15071-A Coruña, Spain*

[c]*Department of Environmental Health, Portuguese National Institute of Health, Rua Alexandre Herculano, 321, 4000-055 Porto, Portugal*

[d]*ISPUP-EPIUnit, Universidade do Porto, Rua das Taipas, 135, 4050-600 Porto, Portugal*

[e]*CIAFEL, Faculdade de Desporto, Universidade do Porto, Rua Dr. Plácido Costa, 91, 4200-450 Porto, Portugal*

[†]These authors contributed equally to the senior authorship of this manuscript.

*Correspondence: Dr. Vanessa Valdiglesias, PhD, University of A Coruña, Toxicology Unit, Research Services Building, Campus Elviña s/n, 15071, A Coruña, Spain. Tel.: +34 981167000 ext. 2680.Fax: +34 981167172. vvaldiglesias@udc.es

Abstract

Iron oxide nanoparticles (ION) have great potential for an increasing number of medical and biological applications, particularly those focused on nervous system. Although ION seem to be biocompatible and present low toxicity, it is imperative to unveil the potential risk for the nervous system associated to their exposure, especially because current data on ION effects on human nervous cells are scarce. Thus, in the present study potential toxicity associated with silica-coated ION (S-ION) exposure was evaluated on human A172 glioblastoma cells. To this aim, a complete toxicological screening testing several exposure times (3 and 24h), nanoparticle concentrations (5-100µg/ml), and culture media (complete and serum-free) was performed to firstly assess S-ION effects at different levels, including cytotoxicity – lactate dehydrogenase assay, analysis of cell cycle and cell death production – and genotoxicity – H2AX phosphorylation assessment, comet assay, micronucleus test and DNA repair competence assay. Results obtained showed that S-ION exhibit certain cytotoxicity, especially in serum-free medium, related to cell cycle disruption and cell death induction. However, scarce genotoxic effects and no alteration of the DNA repair process were observed. Results obtained in this work contribute to increase the knowledge on the impact of ION on the human nervous system cells.

Keywords: iron oxide nanoparticles; A172 cells; neurotoxicity; cytotoxicity; genotoxicity

1 Introduction

Iron oxide nanoparticles (ION) have great potential for an increasing number of medical and biological applications. Due to their size-driven superparamagnetism, they are used in diagnosis, therapeutics and tumor destruction (Revia and Zhang, 2016). ION versatility, together with their physicochemical properties, allow their use as magnetic resonance imaging agents (Abakumov et al., 2015; Gkagkanasiou et al., 2016), heating mediators in hyperthermia-based cancer therapy (Blanco-Andujar et al., 2016; Dan et al., 2015), and molecular cargo in targeted drug (Elzoghby et al., 2016; Thomsen et al., 2015) and gene delivery (Li et al., 2016). Particularly, the design of specific ION for diagnosis and treatment of neurodegenerative and neurovascular diseases has noticeably increased in the last years (Kanwar et al., 2012). However, studies on their possible neurotoxic effects are still scarce and inconclusive, especially in human models (Valdiglesias et al., 2016). The specific use of ION in diagnostics and therapies on the nervous system requires their introduction into the body; given their small size they can cross the blood brain barrier (BBB) and access the brain tissue (Win-Shwe and Fujimaki, 2011). This demonstrated ability of ION to cross the BBB, combined with their high surface area and reactivity, makes the nervous system extremely vulnerable to their potential toxicity. Indeed, previous studies have already demonstrated that ION may induce cytoskeleton impairment, plasmatic membrane disruption, oxidative stress, DNA damage, or alterations in cell signaling pathways in different cells form nervous origin (reviewed in Valdiglesias *et al*., 2016). Still, the lack of robust toxicological screenings, and poor comprehension of predictive paradigms of nanoneurotoxicity are the major obstacles in translating the advancing nanoparticle designs into viable biomedical platforms system (Kim et al., 2013).

Several uncoated and differently coated ION have been reported to be highly biocompatible nanomaterials which do not pose a serious threat to the organism (Laurent et

al., 2014). However, despite being considered as generally safe, potential ION toxicity cannot be completely discarded since results from studies on this regard are often contradictory, and ION effects at certain levels, such as genotoxicity or carcinogenicity, have been poorly addressed (reviewed in Valdiglesias et al., 2014; Revia and Zhang 2016). Most studies reported so far on the consequences of *in vitro* exposure of nervous system cells to different uncoated and coated ION have been performed in neurons, particularly PC12 rat and SH-SY5Y human cells (Deng et al., 2014; Imam et al., 2015; Kiliç et al., 2015; Wu et al., 2013; Wu and Sun, 2011). However, investigating the potential harmful effects of ION on other different nervous system cells (i.e. glial cells: astrocytes, oligodendrocytes and microglial cells) is also relevant since they are involved in neuron support and protection, and alterations in these cells have been implicated in the onset and progression of several neurodegenerative diseases (Barker and Cicchetti, 2014; Cai and Xiao, 2016; Phatnani and Maniatis, 2015). Astrocytes are especially interesting since they are the most abundant brain cell type and the first cellular obstacle ION interact with, and are strategically distributed between the blood vessels and neurons (Geppert et al., 2011). Besides, they seem to play a key role in the etiology of neurodegenerative disorders and, consequently, have been proposed as new targets for the treatment of important neuropathologies such as Alzheimer's disease, amyotrophic lateral sclerosis, and Parkinson's disease (Finsterwald et al., 2015).

For *in vivo* purposes, nanoparticles are required to be biocompatible, water-dispersible, stable in biological media, and uniform in size to maintain the suitable magnetic properties (Chang et al., 2007; Lee et al., 2015). Surface coatings are known generally to influence advantageously nanoparticle features. For this reason, ION are often coated with different organic and inorganic materials to increase their stability and improve their biocompatibility and biodegradability (Al Faraj et al., 2015), decrease their cytotoxicity (Magdolenova et al., 2013), and provide an ample surface for functionalization (Revia and

Zhang 2016). Among all the possible coating materials, silica has several advantages that makes it very suitable for biomedical applications. It can increase ION biocompatibility without affecting magnetic properties, may convert hydrophobic nanoparticles into hydrophilic water-soluble particles, helps to prevent aggregation by improving the nanoparticle chemical stability, and the silanol-terminated surface groups may be modified with various coupling agents to covalently bind to specific ligands reviewed in Andrade *et al.* (2009). All these properties make silica one of the most commonly used agents for ION coating, particularly for bioimaging and biosensing purposes (Alwi et al., 2012). Still, the possible neurotoxicity of silica-coated ION (S-ION), particularly on nervous cells different from neurons, has not been discarded yet.

ION toxicity has been demonstrated to vary considerably and also to depend on cell type and physical-chemical characteristics such as size, shape, presence/type of coating, and stability in biological media (Gupta and Gupta 2005, Mahdavi *et al.* 2013, Strehl *et al.* 2016). In a previous study conducted by our research group (Costa et al., 2015), effects induced by S-ION on viability of A172 glial cells and SH-SY5Y neuronal cells were evaluated. Results showed that S-ION significantly decreased viability, with a moderate effect in the glial cells; besides, a serum-protective effect was observed for both cell lines. Moving forward, the main objective of the present work was to investigate for the very first time the effects of S-ION on human astrocytes (A172 glioblastoma cells), in order to obtain an overview of the risk these nanoparticles may pose when used in biomedical applications on the human nervous system. To this aim, a complete toxicological screening was performed to assess S-ION effects at different levels, including cytotoxicity – cellular membrane impairment, cell cycle disruption and cell death production – and genotoxicity – H2AX phosphorylation, primary DNA damage and micronuclei (MN) induction –, considering also alterations in DNA repair ability and iron ion release capacity.

2 Materials and methods

2.1 Chemicals

Bleomycin (BLM) (CAS no. 9041-93-4) and Triton X-100 (CAS no. 9002-93-1) was purchased from Panreac AppliChem, and mytomycin C (MMC) (CAS no. 50-07-7), camptothecin (Campt) (CAS no. 7689-03-4), hydrogen peroxide (H_2O_2) (CAS no. 7722-84-1), and propidium iodide (PI) (CAS no. 25535-16-4) were purchased from Sigma-Aldrich Co.). BLM, MMC, and PI were dissolved in sterile distilled water, and Campt was dissolved in DMSO prior to use.

2.2 Nanoparticle preparation and characterization

S-ION were synthesized and prepared as stable water suspensions (5 mg/ml) as described by Yi *et al.* (2006). Particle size and morphology were studied by transmission electron microscopy (TEM), while average hydrodynamic size, surface chemistry and zeta potential of nanoparticles in suspension were determined by dynamic light scattering (DLS) in deionized water, complete and serum-free A172 medium (Costa et al., 2015). Prior to each treatment, a stock suspension of S-ION (1 mg/ml) was prepared in serum-free or complete A172 culture medium (see composition below), and was ultrasonicated in a water bath (Branson Sonifier, USA) for 5 min. Serial dilutions were carried out to obtain the different nanoparticle concentrations tested, and sonicated in the water bath for an additional 5 min period.

2.3 Iron ion release from the nanoparticles

In order to quantify the iron ions released from the S-ION, suspensions of 5, 25, 50 y 100 μg/ml were prepared in serum-free or complete cell culture medium and incubated for 3, 6 and 24 h at 37°C in a humidified 5% CO_2 environment. After centrifugation at 14,000 rpm for 30 min, the liquid medium was removed from the S-ION solid phase. Flame atomic absorption spectroscopy (FAAS) (Thermoelemental Solaar S4 v.10.02) was used to quantify

the iron content in the supernatant. Cell culture media without nanoparticles and subjected to the same experimental conditions were used as negative controls.

2.4 Cell culture and S-ION treatments

Human glioblastoma A172 cells were obtained from the European Collection of Cell Cultures and grown in a nutrient mixture composed of DMEM with 1% L-glutamine, 1% antibiotic and antimycotic solution, supplemented with 10% heat inactivated fetal bovine serum (FBS) for complete medium conditions, and of the same mixture without FBS for serum-free (incomplete) medium conditions, in a humidified atmosphere at 37°C with 5% CO_2. Astrocytes were seeded in 96 well-plates (5–8 × 10^4 cells per well) and allowed to adhere for 24 h at 37°C before carrying out the experiments. For each experiment, cells were incubated with four different S-ION concentrations (5, 25, 50 and 100 μg/ml) at 37°C for 3 or 24 h, in serum-free or complete cell culture medium. Our previous results from cell viability assays (Costa et al., 2015) were used to establish these four concentrations and two exposure times. The decrease in viability was lower than 30% in all cases. Regarding physiological significance of the doses tested, the dose range of ION (ferucarbotran, Resovist) required for clinical MR imaging (0.2–0.8 mg Fe/kg body weight) (Reimer and Balzer, 2003) is approximately equivalent to the lower dose tested in this study (2.5-10 μg/ml).

Serum-free and complete cell culture media were used as negative control in all experiments. The following chemicals were employed as positive controls: Campt 10 μM for apoptosis; Triton X-100 1% for lactate dehydrogenase (LDH) assay; MMC 1.5 μM for cell cycle analysis and 15 μM for MN test, BLM 1 μg/ml for γH2AX analysis, and H_2O_2 100 μM for comet assay and 200 μM for DNA repair competence assay.

2.5 Cellular uptake

Transmission electron microscopy (TEM) was used to assess the uptake and intracellular localization of ION in cultured cells. A172 cells were seeded in T25 flasks and

exposed to 25 μg/ml and 100 μg/ml of S-ION dispersed in complete and serum-free media for 3 and 24 h; negative controls (cells with no exposure to nanoparticles) and positive controls (cells exposed to 150 μg/ml of TiO_2 nanoparticles, Sigma reference 637254) were also included in this experiment. After exposure, cells were washed twice with phosphate buffered saline solution, harvested by trypsinization and centrifuged. The pellets were then fixed in 2.5% glutaraldehyde in 0.2 M sodium cacodylate pH 7.2–7.4 for 2 h, post-fixed with 2% osmium tetroxide, dehydrated through graded alcohol solutions and embedded in Epon. Ultrathin sections of 100 nm were mounted on copper grids and contrasted with uranyl acetate and lead citrate and examined with Jeol JEM 1400 transmission electron microscope (Tokyo, Japan) equipped with an energy dispersive X-ray (EDX) spectrometer (Oxford Instruments, Abingdon, UK). Digital images were captured by using a CCD digital camera Orious 1100W (Tokyo, Japan).

2.6 Membrane integrity

A commercial kit (Roche Diagnostics Corp) was used to measure the LDH release in cell culture media, according to the manufacturer's instructions. After exposure, cell culture medium was collected for LDH measurement. Absorption was measured at 490 nm with a reference wavelength of 655 nm using a Cambrex ELx808 microplate reader (Biotek, KC4). Results from positive control experiments (1% Triton X-100) were set as 100% cytotoxicity, and LDH release was calculated as indicated in Valdiglesias *et al.* (2013).

2.7 Cell cycle analysis

The relative cellular DNA content was quantified by flow cytometry in order to determine cell distribution through the different cell cycle phases, according to the method described by Valdiglesias *et al.* (2011). Briefly, after exposure to S-ION, cells were harvested, resuspended in cold phosphate buffer solution (PBS), centrifuged, and fixed with cold 70% (v/v) ethanol (-20º C) overnight at 4º C. For analysis, cells were stained with PI

containing RNase A. DNA content was quantified in at least 10,000 events, as PI signal detected, and the resulting histograms were analyzed by Cell Quest Pro software (Becton Dickinson) to calculate the percentage of occupancy of G_0/G_1, S and G_2/M regions of cell cycle. Complementarily, the subG_1 region, indicative of late stages of apoptosis, was also evaluated.

2.8 Apoptosis and necrosis detection

In order to evaluate the possible induction of cell death by S-ION, the rates of apoptosis and necrosis were measured by means of annexin V/PI double staining, using the Immunostep™ annexin V–FITC apoptosis detection kit according to the manufacturer's recommendations. At least 10,000 events were acquired with a FACSCalibur flow cytometer (Becton Dickinson). Data from annexin V–fluorescein isothiocyanate (FITC) (FL1) and PI (FL2) were analyzed using Cell Quest Pro software (Becton Dickinson) to determine rates of early apoptosis (annexin V positive and PI negative cells) and late apoptosis/necrosis (annexin V and PI positive cells).

2.9 γH2AX assay

The evaluation of H2AX histone phosphorylation after S-ION treatments was assessed as previously described (Sánchez-Flores et al., 2015). Briefly, after nanoparticle exposure, cells were harvested, fixed and permeabilized firstly with cold 1% formaldehyde for 15 min at 4º C, and subsequently with 70% ethanol (-20º C) overnight. Afterwards, cells were incubated with anti-γH2AX antibody and stained with PI containing RNase A. A minimum of 10,000 events were acquired with a FACSCalibur Flow Cytometer (Becton Dickinson). The signal of FL1 and FL2 detectors, corresponding to Alexa Fluor 488 and PI respectively, was analyzed using Cell Quest Pro software (Becton Dickinson).

2.10 Comet assay

Before conducting the comet assay, it was tested whether that S-ION could interfere with the assay methodology, following the procedure described by Magdolenova *et al.* (2012). Briefly, the experiment was performed independently on cells untreated and treated with nanoparticles. In this last case S-ION were added directly to cells just before being embedded in the agarose (at a final concentration of 100 µg/ml, the highest tested), to ensure that nanoparticles were in direct contact with the DNA nucleoids during the lysis step, and then continued with the standard protocol. Since no interference was observed, after treatments with S-ION, the alkaline comet assay was carried out according to Singh et al. (1988), with minor changes (Costa and Teixeira, 2014). In all cases 100 cells per slide were scored (50 from each replicate drop), using Comet IV Software (Perceptive Instruments) for image capture and analysis. The percentage of DNA in the comet tail (%tDNA) was used as DNA damage parameter.

2.11 Micronucleus test

At the end of cell incubations with S-ION, nanoparticles were removed and cells were cultured in fresh medium for an additional period of 48 h, adjusted according to cell cycle duration (33-48 h). Then suspensions of nuclei and MN were prepared and analyzed as previously described (Valdiglesias et al., 2013). Analyses of the final suspensions were carried out in a FACSCalibur Flow Cytometer (Becton Dickinson) evaluating a minimum of 20,000 events in each case.

2.12 DNA repair competence assay

In order to evaluate the effects of S-ION on cellular repair processes, DNA repair competence assay was carried out in A172 astrocytes treated with S-ION at 50 µg/ml. In this assay DNA damage is deliberately induced by a known challenging agent (H_2O_2 in this case). After washing out the challenging agent, repair of the damage induced is allowed during a certain period, and the remaining damage is then evaluated by the comet assay. The difference

between the DNA damage evaluated before and after this period is indicative of the repair ability. Effects of S-ION on cell repair ability were tested by treating the cells in three different phases: (i) phase A (pretreatment), in which cells were incubated at 37° C for 3 or 24 h in the presence or absence of S-ION (50 µg/ml); (ii) phase B (damage induction), in which cells were challenged with H_2O_2 (200 µM) for 5 min at 37°C in the presence or absence of S-ION (50 µg/ml); and (iii) phase C (repair), in which cells were washed out with fresh medium to remove treatment, and incubated with or without S-ION (50 µg/ml) for 30 min at 37°C to allow DNA repair. Alkaline comet assay, as described above, was then performed just after treatment with H_2O_2 (data labeled as *before repair*) and after the repair period (data labeled as *after repair*). In order to confirm that the potential effects observed during phase C (repair) are not due to genotoxicity induced by S-ION, an additional experimental point consisting in an incubation of A172 cells in the presence of S-ION (50 µg/ml) for 30 min was performed.

2.13 Statistical analysis

Statistical analyses were performed using SPSS for Windows statistical package (version 20.0). Differences among groups were tested with Kruskal–Wallis test and Mann-Whitney *U*-test. The associations between two variables were analyzed by Spearman's correlation. A minimum of three independent experiments were performed for every assay, and each experimental condition was run in duplicate. Experimental data were expressed as mean ± standard error and a *P*-value of <0.05 was considered significant.

3 Results

A complete physical-chemical characterization of these nanoparticles was previously carried out (Costa *et al.* 2015). Briefly, S-ION used are spherical particles with an average diameter of 20.2 nm, including core and silica coating; less than 2% of the S-ION surface presents iron, confirming an effective silica coating. Mean hydrodynamic size and zeta potential values in different media demonstrated the suspension stability and low tendency to agglomeration.

3.1 Iron ion release from the nanoparticles

Determination of iron ions in the culture media assessed by FAAS revealed scarce release of ions from the S-ION in serum-free medium regardless exposure time and after 3 h incubation in complete medium. Nevertheless, notable time and concentration-dependent release was observed in complete medium after 6 and 24 h incubations (Fig. 1).

3.2 Cellular uptake

Nanoparticle internalization was analyzed by transmission electron microscopy coupled with EDX in order to confirm nanoparticle composition. Results obtained show that glial cells are able to internalize S-ION at the conditions here tested. Electron-dense deposits were observed within endosomes after 24 h of exposure to S-ION 25 and 100 μg/ml and also after 3 h of exposure to the highest concentration, both in complete and serum-free medium (Fig. 2). These agglomerates were also detected in the intercellular space; signs of apoptosis and necrosis were observed in cells exposed to S-ION.

3.3 Cytotoxicity

3.3.1 Membrane integrity

The possible effect of S-ION on glial cell membrane integrity was analyzed by measuring LDH enzyme release. It was observed that S-ION, regardless of the medium

composition, did not produce significant alterations in membrane integrity, i.e. increases in LDH release, at any condition tested.

3.3.2 Cell cycle analysis

Results obtained in the analysis of the different phases of the cell cycle (G_0/G_1, S, G_2/M) revealed that, in general, S-ION exposure altered the normal progression of A172 cell cycle (Fig. 3). Although no significant differences in the cell distribution in each phase were obtained in the 3 h treatments in complete medium when compared with the control (Fig.3a), there was a statistically significant dose-dependent increase in the S-phase (r=0.406, $P<0.05$) with a simultaneous dose-dependent decrease in the G_0/G_1 phase (r=-0.443, $P<0.05$). After 3 h treatments in serum-free medium (Fig. 3b), significant alterations were observed, mainly in G_0/G_1 (r =-0.594, $P<0.01$) and S phases (r = 0.681; $P<0.01$). Exposure of glial cells to S-ION for 24 h induced significant cell cycle alterations at all concentrations tested, regardless of the medium used (Fig. 3c and 3d). Consequently, positive dose-response relationships were obtained in all phases in complete medium (G_0/G_1: r=-0.864, $P<0.01$; S: r=0.900, $P<0.01$; G_2/M: r=0.481, $P<0.05$), and in G_0/G_1 and S phases in serum-free medium (G_0/G_1: r=-0.733, $P<0.01$; S: r=0.899, $P<0.01$).

In addition, analysis of subG_1 region of the cell cycle distribution was conducted as indicative of late stages of apoptosis (Fig. 4a). S-ION treatment in complete medium induced apoptosis only at the highest concentration and longest exposure time tested. However, a strong dose-dependent cell death generation was observed from 25 µg/ml on in serum-free medium (3 h: r=0.822, $P<0.01$; 24 h: r= 0.880, $P<0.01$).

3.3.3 Apoptosis and necrosis detection

Early apoptosis was assessed by means of annexin V/PI double staining by flow cytometry. Results obtained in complete medium showed significant increases in the percentage of apoptotic cells after treatment with S-ION at the highest concentrations tested,

particularly evident at 24 h exposure but with significant dose-response relationships in both cases (3 h: r=0.426, $P<0.05$, 24 h: r=0.673, $P<0.01$) (Fig. 4b). An even more notable apoptosis induction was observed in serum-free medium, with significant differences with regard to the negative control from 25 µg/ml on and also significant dose-response relationships in both cases (r=0.860, $P<0.01$ for 3 h; r=0.908, $P<0.01$ for 24 h). Furthermore, although necrosis rates obtained in the same analyses were much lower than apoptosis rates, they showed significant dose-dependent increases at the highest concentrations tested (50 and 100 µg/ml) (r=0.558; $P<0.01$) only for the longest exposure time in complete medium (Fig. 4c). In contrast, in serum-free conditions, a dose-dependent relationship was observed at 3 h, with statistically significant increases in the necrosis production from 25 µg/ml on (r=0.832; $P<0.01$), whereas no effect at any dose was observed at 24 h of exposure.

3.4 Genotoxicity

Results obtained from the different genotoxicity assays, i.e. γH2AX, comet and MN assays are shown in Figure 5.

3.4.1 γH2AX assay

Results obtained from analysis of H2AX phosphorylation by flow cytometry are shown in (Fig. 5a). Significant increases in %γH2AX were only observed in A172 cells treated with 50 and 100 µg/ml S-ION for 24 h in complete medium. No effects were observed in complete medium after 3 h exposure and in serum-free medium at any time or dose tested.

3.4.2 Comet assay

When the possible interference between the nanoparticles and the comet methodology was tested, no significant differences were observed between the results obtained in the presence and in the absence of S-ION (100 µg/ml), indicating no nanoparticle interference with any step of the assay, both in complete and serum-free media. Subsequently, increases in primary DNA damage with respect to the controls were observed in S-ION treated cells, at the

highest concentration after 3 h treatment and from 25 μg/ml on after 24 h, regardless of serum presence in the medium (Fig. 5b). Positive dose–response relationships were also found in all cases (r=0.493, $P<0.01$ and r=0.564, $P<0.01$ for 3 h, in complete and serum-free medium, respectively, and r=0.741, $P<0.01$ for 24 h, in complete and serum-free medium, respectively).

3.4.3 MN test

According to MN assay results, no MN induction was observed in glial cells by S-ION treatment at any concentration or exposure time, either in complete or in serum-free medium (Fig. 5c).

3.4.4 DNA repair

As shown in Figure 6, results obtained from the DNA repair competence assay showed a significant decrease in H_2O_2-induced damage after the repair period in all cases, independently of the assay phase in which glial cells were exposed to S-ION. In addition, the absence of damage induction by S-ION when cells were incubated for only 30 min discards any additional DNA damage produced when cells were exposed during the repair phase.

4 Discussion

To guarantee their safety, nanoparticles must not be toxic to the cells at concentrations suitable for magnetic targeting or other biomedical applications. Previous studies indicated that ION exhibit very subtle or no cytotoxic activity when administered at concentrations remaining below 100 µg/ml (Laurent et al., 2014). However, it has also been demonstrated in a number of *in vitro* and *in vivo* studies that ION, both naked and differently coated, may induce adverse effects, even at low doses, through diverse mechanisms such as iron ion release, oxidative stress induction, mitochondrial dysfunction, DNA damage, and alteration of cellular signaling pathways, among others (Revia and Zhang, 2016). Current knowledge on potential neurotoxicity of ION on human nervous cells is scarce and not consistent (reviewed in Valdiglesias *et al.* 2014). On this basis, the present study was designed to elucidate the possible effects of S-ION on human glial cells by evaluating a dose range (5 to 100 µg/ml) and short- and long-term exposure times (3 and 24 h, respectively). In particular, the measurement of membrane integrity, cell cycle progression and apoptosis/necrosis rates were evaluated as indicators of cytotoxicity, whereas primary DNA damage, histone H2AX phosphorylation, MN frequency and DNA repair ability were determined as genotoxicity parameters. ION coated with silica were selected to perform the analyses due to the several advantages of this coating, including negative charge at blood pH or transparent matrix, that make it especially suitable to be employed for medical purposes (Alwi et al., 2012). The A172 cell line employed in this study is an astrocytoma non-tumorigenic and p53 wild-type cell line derived from a human glioblastoma that has been commonly used in *in vitro* studies to elucidate basic neurobiological principles and as a glial model in neurotoxicity testing (Qiang et al., 2009; Sato et al., 2009; Wolff et al., 1999).

The actual entry of nanoparticles into astrocytes was verified prior to toxicity evaluation. Results obtained from TEM revealed the presence of S-ION internalized in A172

astrocytes in all the conditions tested, regardless medium composition or exposure time, demonstrating that these cells may efficiently uptake these nanoparticles. Moreover, S-ION were found to be accumulated in intracellular vesicles, suggesting that endocytic processes are involved in S-ION uptake into astrocytes. Similarly, cultured astrocytes were reported to efficiently accumulate ION with different types of coatings in a time-, concentration- and temperature-dependent manner (Hohnholt et al., 2013).

S-ION did not impair plasmatic membrane integrity at the conditions tested in this study, as demonstrated by the negative results revealed in the assessment of LDH release. Similarly, no significant LDH leakage was observed in SH-SY5Y neuronal cells treated with the same S-ION (Kiliç *et al.* 2015). Previous studies in other cell lines reported membrane damage only at high ION (magnetite) concentration (100 μg/ml) (Watanabe et al., 2013) or long exposure time (maghemite, 24 h) (Rajiv *et al.* 2015). As none of these conditions led to membrane impairment in the current study, results obtained suggest that silica coating prevents membrane damage, and/or that astrocytes are less sensitive to this effect.

The cell cycle machinery is managed by a highly ordered set of events that lead to the division and duplication of the cell (Crosby, 2007). In the presence of DNA damage or cellular stress, cell cycle checkpoint protein p53 triggers cell cycle arrest to provide time for the damage to be repaired or for self-mediated apoptosis (Alarifi et al., 2013). Results obtained from the cell cycle analysis showed important dose-dependent cell cycle alterations induced by S-ION, particularly marked in the 24 h treatments, in which cell cycle of A172 cells resulted altered in all conditions tested, regardless the dose or the medium composition. Still, these effects, included mainly alterations in G_0/G_1 and S phases reflecting a possible mitotic arrest, and were more pronounced in serum-free medium. These results support the previous work of Mahmoudi *et al.* (2012) who also observed similar cell cycle effects in BE(2)-C neurons and A172 astrocytes treated with S-ION (2-32 mM) for 24 h. Similarly,

uncoated magnetite nanoparticles induced a concentration-dependent accumulation of cells in G_2/M phase and of p53 gene expression in neuronal PC12 cells treated for 24 h (100 and 200 µg/ml) (Wu and Sun, 2011). And Mahmoudi *et al.* (2009) observed that uncoated and polyvinyl alcohol-coated ION caused cell cycle arrest in G_0/G_1 phase at 200-400 mM in mouse fibroblast cell line (L929), possibly due to the irreversible DNA damage and repair of oxidative DNA lesions.

Evaluation of apoptosis induced by S-ION exposure was carried out by two approaches; on one hand the analysis of the subG_1 region of the cell cycle as an indicator of DNA fragmentation at the late stages of apoptosis, and on the other hand, by annexin V/PI staining flow cytometric analysis, as a sensitive measure of apoptosis early stages. Results obtained by both methodologies resulted quite similar, with apoptosis induction limited to the highest S-ION doses and longest exposure time in complete medium, but important dose-dependent increases of apoptosis rates observed at both exposure times in serum-free medium. In agreement with our results, Mahmoudi *et al.* (2012) also observed increases in the apoptotic rate (subG1 stage of cell cycle) in BE(2)-C neurons and A172 astrocytes exposed to S-ION for 24 h, and Jeng and Swanson (2006) reported a time-dependent increase of apoptotic Neuro-2A cells after 48 h treatment with carboxyethylsilanetriol-coated ION (50 µg/ml). In general, ION-induced apoptosis was previously described not only in nervous system cells but also in other different cell types, including human A549 lung cells (Watanabe et al., 2013), human Jurkat T lymphocytes (Namvar et al., 2014), or rat lung epithelial cells (Ramesh *et al.* 2012).

Evaluation of cell death by annexin V/PI allowed also to quantify the rate of cells undergoing necrosis together with late apoptosis. In complete medium, S-ION only induced necrosis at the highest doses and longest exposure time; whereas in serum-free medium significant dose-dependent increases were obtained only in the 3 h treatment. Since results

from annexin V/PI analysis and subG$_1$ region are similar, and considering that percentage of annexin V binding +/PI- cells includes not only necrotic but also late apoptotic cells, S-ION seem to induce cell death mainly via the apoptotic pathway. Accordingly, Kiliç *et al.* (2015) did not observe necrosis induction but apoptosis in SH-SY5Y neurons exposed to the same S-ION (100 and 200 µg/ml) for 24 h.

The potential genotoxic effects of S-ION were evaluated by means of three different genotoxicity approaches, namely γH2AX assay, comet assay and MN test. Moreover, DNA repair competence assay was applied to assess possible alterations in the astrocyte DNA repair capacity in presence of S-ION.

Histone H2AX becomes phosphorylated at serine 139 in response to DNA double-strand breaks (DSB), and phosphorylated H2AX (γH2AX) is widely used as a specific and very sensitive marker for this kind of DNA damage (Magdolenova et al., 2014; Rogakou et al., 1998). Still, given its novelty, application of γH2AX assay to ION genotoxicity studies is extremely scarce. According to our previous results, S-ION did not induce DSB in SH-SY5Y cells, either in complete or in serum-free medium (Kiliç *et al.* 2015). In the present study S-ION did not induce H2AX phosphorylation in A172 astrocytes either, except at the highest concentrations after 24 h treatment. Considering the results obtained in the iron ion release from the nanoparticles, the increase detected seems to be more likely due to the indirect effect of iron ions, than to the genotoxic S-ION properties themselves. Presence of iron ions would lead to an imbalance in the Fenton reaction and, consequently, to an increase in oxidative damage, eventually causing breaks in the DNA strands (Luther et al., 2013).

Comet assay was carried out in order to evaluate the possible induction of primary genetic damage by S-ION exposure. Alkaline comet assay is a simple, rapid, and sensitive technique which detects DNA strand breaks, both single and double, alkali-labile sites, abasic sites and serum-free excision repair sites (Kumar and Dhawan, 2013; Lorenzo et al., 2013;

Magdolenova et al., 2014). As several reports previously described the interference of different nanoparticles with the comet assay methodology (Karlsson, 2010; Magdolenova et al., 2012; Stone et al., 2009), the possible interference by S-ION at the highest concentration to be tested was discarded prior to performing the analysis. Subsequently, results from comet assay showed that S-ION induced DNA primary damage in astrocytes only at the highest concentrations after a short exposure period, but from 25 µg/ml on, in a dose-dependent manner, after 24 h treatment. This concentration-dependent increased DNA damage was previously observed in A549 and Hela cells treated with both S-ION (Malvindi et al., 2014) or ION with other different coatings (Bhattacharya *et al.* 2009; Hong *et al.* 2011; Seo *et al.* 2017). However, since the results obtained from γH2AX analysis in this study were mainly negative, this primary DNA damage observed in comet assay seems not be related to DSB but to other kind of DNA damage (e.g. single strand breaks [SSB], abasic sites, alkali-labile sites) more easily repairable.

Micronucleus test was performed to identify possible chromosome alterations induced by exposure to S-ION. MN contain chromosome breaks or whole chromosomes lagged behind during anaphase; consequently MN analysis reveals both clastogenic and aneugenic events (Fenech, 2008). No induction of MN was found in astrocytes exposed to S-ION at any condition tested, indicating on the one hand that S-ION did not induce aneugenic effects on astrocytes. On the other hand, it seems that these cells were able to repair the primary DNA damage initially produced by S-ION exposure, revealed by positive response of comet assay, thus avoiding its fixation as chromosome alterations. A lack of MN production after nanoparticle exposure was obtained in several studies employing different cell lines and ION, as human lymphoblastoid cells treated with uncoated maghemite or with uncoated and dextran-coated magnetite (Singh et al., 2012), Syrian hamster embryo cells treated with naked maghemite and magnetite nanoparticles (Guichard et al., 2012), Chinese hamster lung cells

exposed to glutamic acid-coated (Zhang et al., 2012) and to poly ethylene imine- or poly ethylene glycol-coated ION (Liu et al., 2014).

DNA repair systems are recognized as one of the most important cellular defense mechanisms responsible for DNA integrity. In order to evaluate whether S-ION exposure has some impact on the DNA repair ability of astrocytes, which would lead to increased DNA damage in response to internal or external insults, DNA repair competence assay was carried out with S-ION treatment in different phases. Results obtained showed that S-ION did not interfere with the repair capacity of A172 astrocytes, at any condition tested, since significant decreases in H_2O_2-induced DNA damage, indicative of efficient repair, were observed in the presence of S-ION. These decreases were consistently obtained regardless the moment the incubation with nanoparticles was conducted (before, during or after treatment with the challenging agent H_2O_2), and were also similar to the decrease detected in the absence of S-ION. Studies addressing the potential effects of ION on cellular repair mechanisms are practically inexistent. Our group previously assessed S-ION effects on SH-SY5Y cells repair ability by employing the same approach (Kiliç *et al.* 2015). In that case, S-ION exposure did alter the repair of H_2O_2-induced DNA damage in these cells, with considerably more pronounced effects when serum-free medium was employed. This dissimilar response to S-ION exposure of the two types of nervous system cells indicates, as previously reported, that glioma cells have a more efficient repair capability of induced DNA damage than neurons (Laffon et al., 2017).

All genotoxicity results together indicate that S-ION present a low genotoxic activity, limited to easily repairable DNA damage as demonstrated by the positive results obtained in comet assay together with the negative results from γH2AX and MN assays. In any case, the DNA damage induced by S-ION seems to be repaired, since the repair capacity resulted not altered, and, consequently, it was not fixed in the cells as proved by the lack of MN

production. Besides, all these effects were not dependent on the presence/absence of serum in the medium.

Nevertheless, the quantity of iron ions released from the S-ION depended markedly on the medium composition. While S-ION suspended in serum-free medium were very stable at all conditions tested, suspensions of nanoparticles in complete medium showed a concentration-dependent increase in ion release, particularly noticeable at the longest exposure time. This iron excess may lead to an imbalance in its homeostasis and cause elevated reactive oxygen species (ROS) generation through the Fenton reaction, resulting in oxidative stress which would lead to cytotoxic effects and DNA-damage (Malvindi et al., 2014; Singh et al., 2010; Soenen and De Cuyper, 2010, 2009). Therefore, the iron ion release could help to explain the cytotoxic effects induced by S-ION when complete medium was employed. Since no ion release but cytotoxicity was observed in serum-free medium experiments, other different action mechanisms, for instance those linked to oxidative damage production, should be investigated. Differences in ion release found in our study depending on the medium composition were previously described (Geppert et al., 2012; Hanot et al., 2015; Malvindi et al., 2014). In fact, protein presence has been associated with an increase in dissolution rates of ION through both aqueous complexation and ligand-enhanced dissolution (Nel et al., 2009). Hence, it is possible that the serum proteins favour the silica coating degradation, thus causing a higher iron release from the nanoparticle core. Nevertheless, different issues such as cell type, intracellular medium pH or composition, nanoparticle composition or physical-chemical characteristics such as size, coating or aggregation capacity have been previously suggested to be other main factors influencing the iron release from ION (Geppert et al., 2011, 2009; Paolini et al., 2016; Rosenberg et al., 2012; Singh et al., 2012).

Since ION are often introduced into the organism for biomedical purposes, possible interactions with biological medium components must be considered in their toxicological profile. Indeed, many types of biomolecules – lipids, sugars, and especially serum proteins – are adsorbed onto nanoparticle surface to form the so-called "protein corona" (Bertrand and Leroux, 2012; Lesniak et al., 2010; Mahmoudi et al., 2012b; Monopoli et al., 2012; Nel et al., 2009). This protein binding frequently changes the way cells interact with nanoparticles, because their size and surface characteristics can be altered, leading to functional and structural changes, including interference with enzymatic function (Vertegel et al., 2004). In the present study all experiments were performed in the presence of both complete and serum-free medium, in order to assess the possible influence of this protein corona on the obtained results. Generally speaking, results showed that the absence of serum in the medium had some influence on cytotoxicity of S-ION, resulting in more pronounced cellular effects (cell cycle, apoptosis and necrosis). These findings are in accordance with our previous observations of higher decreases in viability induced by S-ION in both A172 and SH-SY5Y cells in serum-free medium (Costa *et al.* 2015), and support a possible protective effect of the protein corona on the cytotoxicity induced by nanoparticles previously suggested by other authors (Mahmoudi et al., 2012, 2011; Nel et al., 2009). Nevertheless, in general no notable differences in genotoxicity induction or DNA repair alterations were found between complete and serum-free medium.

5 Conclusions

Despite the increasing use of ION in biomedical applications, many current studies on toxicity assessment are far from reaching a conclusion and providing guidance for their safe use. Hence, more comprehensive methodological approaches need to be addressed for the evaluation of ION, in order to better understand the potential risk they may pose. In the present study genotoxicity and cytotoxicity associated with S-ION exposure were evaluated in glial cells by a battery of assays. Results obtained showed that S-ION exhibit certain cytotoxicity, especially in serum-free medium, related to cell cycle disruption and cell death induction. However, S-ION presented scarce genotoxic effects, not dependent on medium composition and easily repairable. Moreover, the primary DNA damage was only related to DSB at the highest concentrations and longest time tested, probably associated with the increase in iron release in complete medium. Negative results in MN test indicate (i) no aneugenic effects and (ii) that the previously mentioned DNA strand breaks were not fixed upon cell division. No effects on the DNA repair systems were observed.

Results obtained in this work contribute to increase the knowledge on the impact of ION on the human nervous system cells. Still, further investigations are required to clarify the possible role of ROS production and oxidative stress on S-ION toxicity, and the interaction of serum proteins with ION surface.

Acknowledgements

This work was funded by Xunta de Galicia (ED431B 2016/013). V. Valdiglesias was supported by a Xunta de Galicia postdoctoral fellowship (reference ED481B 2016/190-0). N. Fernández-Bertólez was supported by an INDITEX-UDC fellowship. F. Brandão is supported by the grant SFRH/BD/101060/2014, funded by FCT (financing subsided by national fund of MCTES). Authors would also like to acknowledge COST Action CA15132 "The comet assay as a human biomonitoring tool (hCOMET)".

Conflict of interest

The authors declare that they have no conflict of interests.

References

Abakumov, M.A., Nukolova, N. V., Sokolsky-Papkov, M., Shein, S.A., Sandalova, T.O., Vishwasrao, H.M., Grinenko, N.F., Gubsky, I.L., Abakumov, A.M., Kabanov, A. V., Chekhonin, V.P., 2015. VEGF-targeted magnetic nanoparticles for MRI visualization of brain tumor. Nanomedicine Nanotechnology, Biol. Med. 11, 825–833. https://doi.org/10.1016/j.nano.2014.12.011

Al Faraj, A., Shaik, A.P., Shaik, A.S., 2015. Effect of surface coating on the biocompatibility and in vivo MRI detection of iron oxide nanoparticles after intrapulmonary administration. Nanotoxicology 9, 825–34. https://doi.org/10.3109/17435390.2014.980450

Alarifi, S., Ali, D., Alkahtani, S., Verma, A., Ahamed, M., Ahmed, M., Alhadlaq, H.A., 2013. Induction of oxidative stress, DNA damage, and apoptosis in a malignant human skin melanoma cell line after exposure to zinc oxide nanoparticles. Int. J. Nanomedicine 8, 983–993. https://doi.org/10.2147/IJN.S42028

Alwi, R., Telenkov, S., Mandelis, A., Leshuk, T., Gu, F., Oladepo, S., Michaelian, K., 2012. Silica-coated super paramagnetic iron oxide nanoparticles (SPION) as biocompatible contrast agent in biomedical photoacoustics. Biomed. Opt. Express 3, 2500–9. https://doi.org/10.1364/BOE.3.002500

Andrade, A.L., Souza, D.M., Pereira, M.C., Fabris, J.D., Domingues, R.Z., 2009. Synthesis and characterization of magnetic nanoparticles coated with silica through a sol-gel approach. Cerâmica 55, 420–424. https://doi.org/10.1590/S0366-69132009000400013

Barker, R.A., Cicchetti, F., 2014. Neurodegenerative disorders: The glia way forward. Front. Pharmacol. 5 JUL, 157. https://doi.org/10.3389/fphar.2014.00157

Bertrand, N., Leroux, J.-C., 2012. The journey of a drug-carrier in the body: an anatomo-physiological perspective. J. Control. Release 161, 152–63.

https://doi.org/10.1016/j.jconrel.2011.09.098

Bhattacharya, K., Davoren, M., Boertz, J., Schins, R.P., Hoffmann, E., Dopp, E., 2009. Titanium dioxide nanoparticles induce oxidative stress and DNA-adduct formation but not DNA-breakage in human lung cells. Part. Fibre Toxicol. 6, 17. https://doi.org/10.1186/1743-8977-6-17

Blanco-Andujar, C., Walter, A., Cotin, G., Bordeianu, C., Mertz, D., Felder-Flesch, D., Begin-Colin, S., 2016. Design of iron oxide-based nanoparticles for MRI and magnetic hyperthermia. Nanomedicine 11, 1889–1910. https://doi.org/10.2217/nnm-2016-5001

Cai, Z., Xiao, M., 2016. Oligodendrocytes and Alzheimer's disease. Int. J. Neurosci. 126, 97–104. https://doi.org/10.3109/00207454.2015.1025778

Chang, P.C., Liu, B.Y., Liu, C.M., Chou, H.H., Ho, M.H., Liu, H.C., Wang, D.M., Hou, L.T., 2007. Bone tissue engineering with novel rhBMP2-PLLA composite scaffolds. J. Biomed. Mater. Res. - Part A 81, 771–780. https://doi.org/10.1002/jbm.a.31031

Costa, C., Brandão, F., Bessa, M.J., Costa, S., Valdiglesias, V., Kiliç, G., Fernández-Bertólez, N., Quaresma, P., Pereira, E., Pásaro, E., Laffon, B., Teixeira, J.P., 2015. In vitro cytotoxicity of superparamagnetic iron oxide nanoparticles on neuronal and glial cells. Evaluation of nanoparticle interference with viability tests. J. Appl. Toxicol. 36, 361–372. https://doi.org/10.1002/jat.3213

Costa, S., Paulo Teixeira, J., Schmezer, P., 2014. Comet Assay. Encycl. Toxicol. 1, 1020–1023. https://doi.org/10.1016/B978-0-12-386454-3.01072-1

Crosby, M.E., 2007. Cell Cycle: Principles of Control. Yale J. Biol. Med. 80, 141–142. https://doi.org/10.1093/icb/icm066

Dan, M., Bae, Y., Pittman, T.A., Yokel, R.A., 2015. Alternating Magnetic Field-Induced Hyperthermia Increases Iron Oxide Nanoparticle Cell Association/Uptake and Flux in Blood-Brain Barrier Models. Pharm. Res. 32, 1615–1625.

https://doi.org/10.1007/s11095-014-1561-6

Deng, M., Huang, Z., Zou, Y., Yin, G., Liu, J., Gu, J., 2014. Fabrication and neuron cytocompatibility of iron oxide nanoparticles coated with silk-fibroin peptides. Colloids Surfaces B Biointerfaces 116, 465–471. https://doi.org/10.1016/j.colsurfb.2014.01.021

Dissanayake, N.M., Current, K.M., Obare, S.O., 2015. Mutagenic Effects of Iron Oxide Nanoparticles on Biological Cells. Int. J. Mol. Sci. 16, 23482–516. https://doi.org/10.3390/ijms161023482

Elzoghby, A.O., Hemasa, A.L., Freag, M.S., 2016. Hybrid protein-inorganic nanoparticles: From tumor-targeted drug delivery to cancer imaging. J. Control. Release 243, 303–322. https://doi.org/10.1016/j.jconrel.2016.10.023

Fenech, M., 2008. The micronucleus assay determination of chromosomal level DNA damage. Methods Mol. Biol. 410, 185–216. https://doi.org/10.1007/978-1-59745-548-0_12

Finsterwald, C., Magistretti, P., Lengacher, S., 2015. Astrocytes: New Targets for the Treatment of Neurodegenerative Diseases. Curr. Pharm. Des. 21, 3570–3581. https://doi.org/10.2174/1381612821666150710144502

Geppert, M., Hohnholt, M., Gaetjen, L., Grunwald, I., Bäumer, M., Dringen, R., 2009. Accumulation of iron oxide nanoparticles by cultured brain astrocytes. J. Biomed. Nanotechnol. 5, 285–93. https://doi.org/10.1016/j.neuint.2014.12.005

Geppert, M., Hohnholt, M.C., Nürnberger, S., Dringen, R., 2012. Ferritin up-regulation and transient ROS production in cultured brain astrocytes after loading with iron oxide nanoparticles. Acta Biomater. 8, 3832–3839. https://doi.org/10.1016/j.actbio.2012.06.029

Geppert, M., Hohnholt, M.C., Thiel, K., Nürnberger, S., Grunwald, I., Rezwan, K., Dringen, R., 2011. Uptake of dimercaptosuccinate-coated magnetic iron oxide nanoparticles by

cultured brain astrocytes. Nanotechnology 22, 145101. https://doi.org/10.1088/0957-4484/22/14/145101

Gkagkanasiou, M., Ploussi, A., Gazouli, M., Efstathopoulos, E.P., 2016. USPIO-Enhanced MRI Neuroimaging: A Review. J. Neuroimaging 26, 161–168. https://doi.org/10.1111/jon.12318

Guichard, Y., Schmit, J., Darne, C., Gaté, L., Goutet, M., Rousset, D., Rastoix, O., Wrobel, R., Witschger, O., Martin, A., Fierro, V., Binet, S., 2012. Cytotoxicity and genotoxicity of nanosized and microsized titanium dioxide and iron oxide particles in syrian hamster embryo cells, in: Annals of Occupational Hygiene. pp. 631–644. https://doi.org/10.1093/annhyg/mes006

Gupta, A.K., Gupta, M., 2005a. Cytotoxicity suppression and cellular uptake enhancement of surface modified magnetic nanoparticles. Biomaterials 26, 1565–1573. https://doi.org/10.1016/j.biomaterials.2004.05.022

Gupta, A.K., Gupta, M., 2005b. Synthesis and surface engineering of iron oxide nanoparticles for biomedical applications. Biomaterials 26, 3995–4021. https://doi.org/10.1016/j.biomaterials.2004.10.012

Hanot, C., Choi, Y., Anani, T., Soundarrajan, D., David, A., 2015. Effects of Iron-Oxide Nanoparticle Surface Chemistry on Uptake Kinetics and Cytotoxicity in CHO-K1 Cells. Int. J. Mol. Sci. 17, 54. https://doi.org/10.3390/ijms17010054

Hohnholt, M.C., Geppert, M., Luther, E.M., Petters, C., Bulcke, F., Dringen, R., 2013. Handling of Iron Oxide and Silver Nanoparticles by Astrocytes. Neurochem. Res. 38, 227–239. https://doi.org/10.1007/s11064-012-0930-y

Hong, S.C., Lee, J.H., Lee, J., Kim, H.Y., Park, J.Y., Cho, J., Lee, J., Han, D.W., 2011. Subtle cytotoxicity and genotoxicity differences in superparamagnetic iron oxide nanoparticles coated with various functional groups. Int. J. Nanomedicine 6, 3219–3231.

https://doi.org/10.2147/IJN.S26355

Imam, S.Z., Lantz-McPeak, S.M., Cuevas, E., Rosas-Hernandez, H., Liachenko, S., Zhang, Y., Sarkar, S., Ramu, J., Robinson, B.L., Jones, Y., Gough, B., Paule, M.G., Ali, S.F., Binienda, Z.K., 2015. Iron Oxide Nanoparticles Induce Dopaminergic Damage: In vitro Pathways and In Vivo Imaging Reveals Mechanism of Neuronal Damage. Mol. Neurobiol. 52, 913–926. https://doi.org/10.1007/s12035-015-9259-2

Jeng, H.A., Swanson, J., 2006. Toxicity of metal oxide nanoparticles in mammalian cells. J. Environ. Sci. Heal. Part a-Toxic/Hazardous Subst. Environ. Eng. 41, 2699–2711. https://doi.org/10.1080/10934520600966177

Joris, F., Valdepérez, D., Pelaz, B., Soenen, S.J., Manshian, B.B., Parak, W.J., De Smedt, S.C., Raemdonck, K., 2016. The impact of species and cell type on the nanosafety profile of iron oxide nanoparticles in neural cells. J. Nanobiotechnology 14, 69. https://doi.org/10.1186/s12951-016-0220-y

Kanwar, J.R., Sriramoju, B., Kanwar, R.K., 2012. Neurological disorders and therapeutics targeted to surmount the blood-brain barrier. Int. J. Nanomedicine 7, 3259–3278. https://doi.org/10.2147/IJN.S30919

Karlsson, H.L., 2010. The comet assay in nanotoxicology research. Anal. Bioanal. Chem. 398, 651–666. https://doi.org/10.1007/s00216-010-3977-0

Kiliç, G., Costa, C., Fernández-Bertólez, N., Pásaro, E., Teixeira, J.P., Laffon, B., Valdiglesias, V., 2015. In vitro toxicity evaluation of silica-coated iron oxide nanoparticles in human SHSY5Y neuronal cells. Toxicol. Res. 5, 235–247. https://doi.org/10.1039/C5TX00206K

Kim, Y., Kong, S.D., Chen, L.-H., Pisanic, T.R., Jin, S., Shubayev, V.I., 2013. In vivo nanoneurotoxicity screening using oxidative stress and neuroinflammation paradigms. Nanomedicine Nanotechnology, Biol. Med. 9, 1057–1066.

https://doi.org/10.1016/j.nano.2013.05.002

Kumar, A., Dhawan, A., 2013. Genotoxic and carcinogenic potential of engineered nanoparticles: an update. Arch. Toxicol. 87, 1883–1900. https://doi.org/10.1007/s00204-013-1128-z

Laffon, B., Fernández-Bertólez, N., Costa, C., Pásaro, E., Valdiglesias, V., 2017. Comparative study of human neuronal and glial cell sensitivity for in vitro neurogenotoxicity testing. Food Chem. Toxicol. 102, 120–128. https://doi.org/10.1016/j.fct.2017.02.005

Laurent, S., Saei, A.A., Behzadi, S., Panahifar, A., Mahmoudi, M., 2014. Superparamagnetic iron oxide nanoparticles for delivery of therapeutic agents: opportunities and challenges. Expert Opin. Drug Deliv. 11, 1449–70. https://doi.org/10.1517/17425247.2014.924501

Lee, S.H., Lee, D.H., Jung, H., Han, Y.-S., Kim, T.-H., Yang, W., 2015. Magnetic properties of SiO2-coated iron oxide nanoparticles studied by polarized small angle neutron scattering. Curr. Appl. Phys. 15, 915–919. https://doi.org/10.1016/j.cap.2015.04.003

Lesniak, A., Campbell, A., Monopoli, M.P., Lynch, I., Salvati, A., Dawson, K.A., 2010. Serum heat inactivation affects protein corona composition and nanoparticle uptake. Biomaterials 31, 9511–9518. https://doi.org/10.1016/j.biomaterials.2010.09.049

Lewinski, N., Colvin, V., Drezek, R., 2008. Cytotoxicity of nanopartides. Small 4, 26–49. https://doi.org/10.1002/smll.200700595

Li, X., Wei, J., Aifantis, K.E., Fan, Y., Feng, Q., Cui, F.Z., Watari, F., 2016. Current investigations into magnetic nanoparticles for biomedical applications. J. Biomed. Mater. Res. - Part A 104, 1285–1296. https://doi.org/10.1002/jbm.a.35654

Liu, Y., Xia, Q., Liu, Y., Zhang, S., Cheng, F., Zhong, Z., Wang, L., Li, H., Xiao, K., 2014. Genotoxicity assessment of magnetic iron oxide nanoparticles with different particle sizes and surface coatings. Nanotechnology 25, 425101. https://doi.org/10.1088/0957-

4484/25/42/425101

Lorenzo, Y., Costa, S., Collins, A.R., Azqueta, A., 2013. The comet assay, DNA damage, DNA repair and cytotoxicity: Hedgehogs are not always dead. Mutagenesis 28, 427–432. https://doi.org/10.1093/mutage/get018

Luther, E.M., Petters, C., Bulcke, F., Kaltz, A., Thiel, K., Bickmeyer, U., Dringen, R., 2013. Endocytotic uptake of iron oxide nanoparticles by cultured brain microglial cells. Acta Biomater. 9, 8454–8465. https://doi.org/10.1016/j.actbio.2013.05.022

Magdolenova, Z., Collins, A., Kumar, A., Dhawan, A., Stone, V., Dusinska, M., 2014. Mechanisms of genotoxicity. A review of in vitro and in vivo studies with engineered nanoparticles. Nanotoxicology 8, 233–78. https://doi.org/10.3109/17435390.2013.773464

Magdolenova, Z., Drlickova, M., Henjum, K., Rundén-Pran, E., Tulinska, J., Bilanicova, D., Pojana, G., Kazimirova, A., Barancokova, M., Kuricova, M., Liskova, A., Staruchova, M., Ciampor, F., Vavra, I., Lorenzo, Y., Collins, A., Rinna, A., Fjellsbø, L., Volkovova, K., Marcomini, A., Amiry-Moghaddam, M., Dusinska, M., 2013. Coating-dependent induction of cytotoxicity and genotoxicity of iron oxide nanoparticles. Nanotoxicology 9, 44–56. https://doi.org/10.3109/17435390.2013.847505

Magdolenova, Z., Lorenzo, Y., Collins, A., Dusinska, M., 2012. Can Standard Genotoxicity Tests be Applied to Nanoparticles? J. Toxicol. Environ. Heal. Part A 75, 800–806. https://doi.org/10.1080/15287394.2012.690326

Mahdavi, M., Ahmad, M. Bin, Haron, M.J., Namvar, F., Nadi, B., Rahman, M.Z.A., Amin, J., 2013. Synthesis, Surface Modification and Characterisation of Biocompatible Magnetic Iron Oxide Nanoparticles for Biomedical Applications. Molecules 18, 7533–7548. https://doi.org/10.3390/molecules18077533

Mahmoudi, M., Hofmann, H., Rothen-Rutishauser, B., Petri-Fink, A., 2012a. Assessing the In

Vitro and In Vivo Toxicity of Superparamagnetic Iron Oxide Nanoparticles. Chem. Rev. 112, 2323–2338. https://doi.org/10.1021/cr2002596

Mahmoudi, M., Lynch, I., Ejtehadi, M.R., Monopoli, M.P., Bombelli, F.B., Laurent, S., 2011. Protein−Nanoparticle Interactions: Opportunities and Challenges. Chem. Rev. 111, 5610–5637. https://doi.org/10.1021/cr100440g

Mahmoudi, M., Saeedi-Eslami, S.N., Shokrgozar, M.A., Azadmanesh, K., Hassanlou, M., Kalhor, H.R., Burtea, C., Rothen-Rutishauser, B., Laurent, S., Sheibani, S., Vali, H., 2012b. Cell "vision": complementary factor of protein corona in nanotoxicology. Nanoscale 4, 5461. https://doi.org/10.1039/c2nr31185b

Mahmoudi, M., Simchi, A., Imani, M., 2009. Cytotoxicity of uncoated and polyvinyl alcohol coated superparamagnetic iron oxide nanoparticles. J. Phys. Chem. C 113, 9573–9580. https://doi.org/10.1021/jp9001516

Malvindi, M.A., De Matteis, V., Galeone, A., Brunetti, V., Anyfantis, G.C., Athanassiou, A., Cingolani, R., Pompa, P.P., 2014. Toxicity assessment of silica coated iron oxide nanoparticles and biocompatibility improvement by surface engineering. PLoS One 9, e85835. https://doi.org/10.1371/journal.pone.0085835

Migliore, L., Uboldi, C., Di Bucchianico, S., Coppedè, F., 2015. Nanomaterials and neurodegeneration. Environ. Mol. Mutagen. 56, 149–170. https://doi.org/10.1002/em.21931

Monopoli, M.P., Åberg, C., Salvati, A., Dawson, K.A., 2012. Biomolecular coronas provide the biological identity of nanosized materials. Nat. Nanotechnol. 7, 779–786. https://doi.org/10.1038/nnano.2012.207

Namvar, F., Rahman, H.S., Mohamad, R., Baharara, J., Mahdavi, M., Amini, E., Chartrand, M.S., Yeap, S.K., 2014. Cytotoxic effect of magnetic iron oxide nanoparticles synthesized via seaweed aqueous extract. Int. J. Nanomedicine 9, 2479–2488.

https://doi.org/10.2147/IJN.S59661

Nel, A.E., Mädler, L., Velegol, D., Xia, T., Hoek, E.M. V., Somasundaran, P., Klaessig, F., Castranova, V., Thompson, M., 2009. Understanding biophysicochemical interactions at the nano–bio interface. Nat. Mater. 8, 543–557. https://doi.org/10.1038/nmat2442

Paolini, A., Guarch, C.P., Ramos-López, D., de Lapuente, J., Lascialfari, A., Guari, Y., Larionova, J., Long, J., Nano, R., 2016. Rhamnose-coated superparamagnetic iron-oxide nanoparticles: An evaluation of their in vitro cytotoxicity, genotoxicity and carcinogenicity. J. Appl. Toxicol. 36, 510–520. https://doi.org/10.1002/jat.3273

Park, E.J., Umh, H.N., Kim, S.W., Cho, M.H., Kim, J.H., Kim, Y., 2014. ERK pathway is activated in bare-FeNPs-induced autophagy. Arch. Toxicol. 88, 323–336. https://doi.org/10.1007/s00204-013-1134-1

Petters, C., Irrsack, E., Koch, M., Dringen, R., 2014. Uptake and Metabolism of Iron Oxide Nanoparticles in Brain Cells. Neurochem. Res. 39, 1648–1660. https://doi.org/10.1007/s11064-014-1380-5

Phatnani, H., Maniatis, T., 2015. Astrocytes in neurodegenerative disease. Cold Spring Harb. Perspect. Biol. 7, 1–18. https://doi.org/10.1101/cshperspect.a020628

Qiang, L., Yang, Y., Ma, Y.-J., Chen, F.-H., Zhang, L.-B., Liu, W., Qi, Q., Lu, N., Tao, L., Wang, X.-T., You, Q.-D., Guo, Q.-L., 2009. Isolation and characterization of cancer stem like cells in human glioblastoma cell lines. Cancer Lett. 279, 13–21. https://doi.org/10.1016/j.canlet.2009.01.016

Rajiv, S., Jerobin, J., Saranya, V., Nainawat, M., Sharma, A., Makwana, P., Gayathri, C., Bharath, L., Singh, M., Kumar, M., Mukherjee, A., Chandrasekaran, N., 2015. Comparative cytotoxicity and genotoxicity of cobalt (II, III) oxide, iron (III) oxide, silicon dioxide, and aluminum oxide nanoparticles on human lymphocytes in vitro. Hum. Exp. Toxicol. 35, 170–183. https://doi.org/10.1177/0960327115579208

Ramesh, V., Ravichandran, P., Copeland, C.L., Gopikrishnan, R., Biradar, S., Goornavar, V., Ramesh, G.T., Hall, J.C., 2012. Magnetite induces oxidative stress and apoptosis in lung epithelial cells. Mol. Cell. Biochem. 363, 225–234. https://doi.org/10.1007/s11010-011-1174-x

Reimer, P., Balzer, T., 2003. Ferucarbotran (Resovist): a new clinically approved RES-specific contrast agent for contrast-enhanced MRI of the liver: properties, clinical development, and applications. Eur. Radiol. 13, 1266–1276. https://doi.org/10.1007/s00330-002-1721-7

Revia, R.A., Zhang, M., 2016. Magnetite nanoparticles for cancer diagnosis, treatment, and treatment monitoring: Recent advances. Mater. Today 19, 157–168. https://doi.org/10.1016/j.mattod.2015.08.022

Rogakou, E.P., Pilch, D.R., Orr, A.H., Ivanova, V.S., Bonner, W.M., 1998. DNA Double-stranded Breaks Induce Histone H2AX Phosphorylation on Serine 139. J. Biol. Chem. 273, 5858–5868. https://doi.org/10.1074/jbc.273.10.5858

Rosenberg, J.T., Sachi-Kocher, A., Davidson, M.W., Grant, S.C., 2012. Intracellular SPIO labeling of microglia: High field considerations and limitations for MR microscopy. Contrast Media Mol. Imaging 7, 121–129. https://doi.org/10.1002/cmmi.470

Sánchez-Flores, M., Pásaro, E., Bonassi, S., Laffon, B., Valdiglesias, V., 2015. γH2AX Assay as DNA Damage Biomarker for Human Population Studies: Defining Experimental Conditions. Toxicol. Sci. 144, 406–413. https://doi.org/10.1093/toxsci/kfv011

Sato, Y., Kurose, A., Ogawa, A., Ogasawara, K., Traganos, F., Darzynkiewicz, Z., Sawai, T., 2009. Diversity of DNA damage response of astrocytes and glioblastoma cell lines with various p53 status to treatment with etoposide and temozolomide. Cancer Biol. Ther. 8, 452–457. https://doi.org/10.4161/cbt.8.5.7740

Seo, D.Y., Jin, M., Ryu, J.-C., Kim, Y.-J., 2017. Investigation of the genetic toxicity by

dextran-coated superparamagnetic iron oxide nanoparticles (SPION) in HepG2 cells using the comet assay and cytokinesis-block micronucleus assay. Toxicol. Environ. Health Sci. 9, 23–29. https://doi.org/10.1007/s13530-017-0299-z

Singh, N., Jenkins, G.J.S., Asadi, R., Doak, S.H., 2010. Potential toxicity of superparamagnetic iron oxide nanoparticles (SPION). Nano Rev. 1, 5358. https://doi.org/10.3402/nano.v1i0.5358

Singh, N., Jenkins, G.J.S., Nelson, B.C., Marquis, B.J., Maffeis, T.G.G., Brown, A.P., Williams, P.M., Wright, C.J., Doak, S.H., 2012. The role of iron redox state in the genotoxicity of ultrafine superparamagnetic iron oxide nanoparticles. Biomaterials 33, 163–170. https://doi.org/10.1016/j.biomaterials.2011.09.087

Singh, N.P., McCoy, M.T., Tice, R.R., Schneider, E.L., 1988. A simple technique for quantitation of low levels of DNA damage in individual cells. Exp. Cell Res. 175, 184–191. https://doi.org/10.1016/0014-4827(88)90265-0

Soenen, S.J.H., De Cuyper, M., 2010. Assessing iron oxide nanoparticle toxicity in vitro : current status and future prospects. Nanomedicine 5, 1261–1275. https://doi.org/10.2217/nnm.10.106

Soenen, S.J.H., De Cuyper, M., 2009. Assessing cytotoxicity of (iron oxide-based) nanoparticles: an overview of different methods exemplified with cationic magnetoliposomes. Contrast Media Mol. Imaging 4, 207–19. https://doi.org/10.1002/cmmi.282

Stone, V., Johnston, H., Schins, R.P.F., 2009. Development of in vitro systems for nanotoxicology: methodological considerations. Crit. Rev. Toxicol. 39, 613–626. https://doi.org/10.1080/10408440903120975

Strehl, C., Maurizi, L., Gaber, T., Hoff, P., Broschard, T., Poole, A.R., Hofmann, H., Buttgereit, F., 2016. Modification of the surface of superparamagnetic iron oxide

nanoparticles to enable their safe application in humans. Int. J. Nanomedicine Volume 11, 5883–5896. https://doi.org/10.2147/IJN.S110579

Thomsen, L.B., Thomsen, M.S., Moos, T., 2015. Targeted drug delivery to the brain using magnetic nanoparticles. Ther. Deliv. 6, 1145–1155. https://doi.org/10.4155/tde.15.56

Totsuka, Y., Ishino, K., Kato, T., Goto, S., Tada, Y., Nakae, D., Watanabe, M., Wakabayashi, K., 2014. Magnetite Nanoparticles Induce Genotoxicity in the Lungs of Mice via Inflammatory Response. Nanomaterials 4, 175–188. https://doi.org/10.3390/nano4010175

Valdiglesias, V., Costa, C., Kiliç, G., Costa, S., Pásaro, E., Laffon, B., Teixeira, J.P., Paulo, J., 2013. Neuronal cytotoxicity and genotoxicity induced by zinc oxide nanoparticles. Environ. Int. 55, 92–100. https://doi.org/10.1016/j.envint.2013.02.013

Valdiglesias, V., Fernández-Bertólez, N., Kiliç, G., Costa, C., Costa, S., Fraga, S., Bessa, M.J., Pásaro, E., Teixeira, J.P., Laffon, B., 2016. Are iron oxide nanoparticles safe? Current knowledge and future perspectives. J. Trace Elem. Med. Biol. 38, 53–63. https://doi.org/10.1016/j.jtemb.2016.03.017

Valdiglesias, V., Kilic, G., Costa, C., Fernandez-Bertolez, N., Pasaro, E., Teixeira, J.P., Laffon, B., 2014. Effects of iron oxide nanoparticles: cytotoxicity, genotoxicity, developmental toxicity, and neurotoxicity. Environ. Mol. Mutagen. 56, 125–148. https://doi.org/10.1002/em.21909

Valdiglesias, V., Laffon, B., Pásaro, E., Méndez, J., 2011. Okadaic acid induces morphological changes, apoptosis and cell cycle alterations in different human cell types. J. Environ. Monit. 13, 1831–40. https://doi.org/10.1039/c0em00771d

Vertegel, A.A., Siegel, R.W., Dordick, J.S., 2004. Silica nanoparticle size influences the structure and enzymatic activity of adsorbed lysozyme. Langmuir 20, 6800–6807. https://doi.org/10.1021/la0497200

Watanabe, M., Yoneda, M., Morohashi, A., Hori, Y., Okamoto, D., Sato, A., Kurioka, D., Nittami, T., Hirokawa, Y., Shiraishi, T., Kawai, K., Kasai, H., Totsuka, Y., 2013. Effects of Fe3O4 magnetic nanoparticles on A549 cells. Int. J. Mol. Sci. 14, 15546–15560. https://doi.org/10.3390/ijms140815546

Win-Shwe, T.-T., Fujimaki, H., 2011. Nanoparticles and neurotoxicity. Int. J. Mol. Sci. 12, 6267–80. https://doi.org/10.3390/ijms12096267

Wolff, J.E.A., Trilling, T., Mölenkamp, G., Egeler, R.M., Jürgens, H., 1999. Chemosensitivity of glioma cells in vitro: a meta analysis. J. Cancer Res. Clin. Oncol. 125, 481–486. https://doi.org/10.1007/s004320050305

Wu, J., Ding, T., Sun, J., 2013. Neurotoxic potential of iron oxide nanoparticles in the rat brain striatum and hippocampus. Neurotoxicology 34, 243–253. https://doi.org/10.1016/j.neuro.2012.09.006

Wu, J., Sun, J., 2011. Investigation on mechanism of growth arrest induced by iron oxide nanoparticles in PC12 cells. J. Nanosci. Nanotechnol. 11, 11079–11083. https://doi.org/10.1166/jnn.2011.394

Yi, D.K., Lee, S.S., Papaefthymiou, G.C., Ying, J.Y., 2006. Nanoparticle architectures templated by SiO 2/Fe 2O 3 nanocomposites. Chem. Mater. 18, 614–619. https://doi.org/10.1021/cm0512979

Zhang, T., Qian, L., Tang, M., Xue, Y., Kong, L., Zhang, S., Pu, Y., 2012. Evaluation on Cytotoxicity and Genotoxicity of the L-Glutamic Acid Coated Iron Oxide Nanoparticles. J. Nanosci. Nanotechnol. 12, 2866–2873. https://doi.org/10.1166/jnn.2012.5763

Figures

Figure 1.

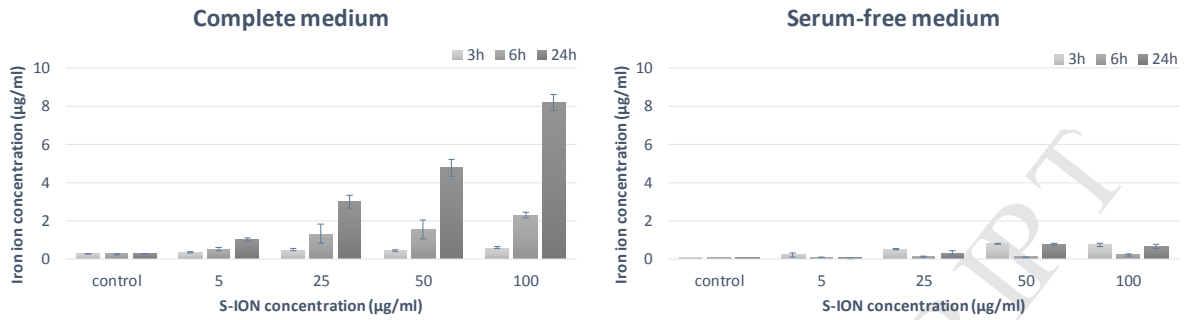

Fig. 1. Analysis of iron ion release from S-ION in complete and serum-free cell culture medium. Bars represent mean ± standard error.

Figure 2.

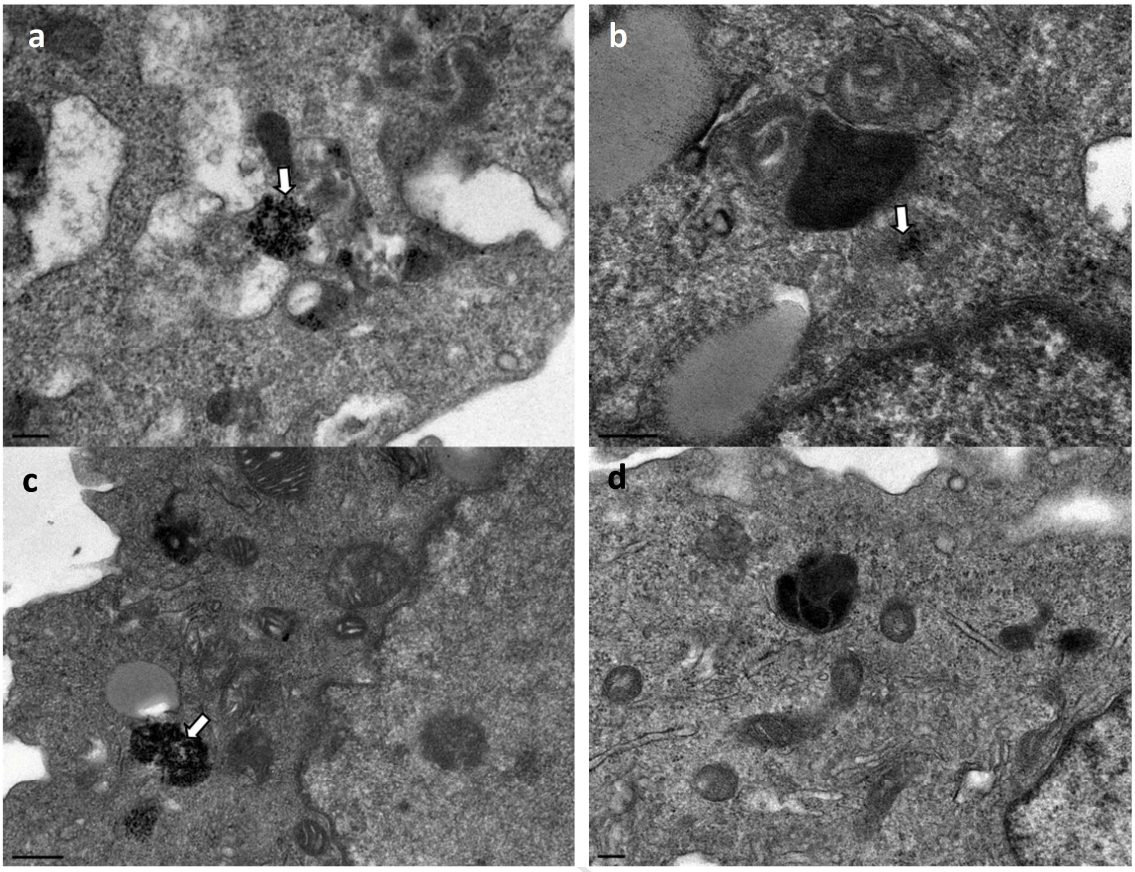

Fig. 2. Transmission electron micrographs of A172 cells incubated with 100 μg/ml of S-ION for 3 h in complete (a) and serum-free (b) medium, and for 24 h in complete (c) medium, showing nanoparticle internalization (arrows indicate S-ION agglomerates). (d) Control A172 cells (not exposed to S-ION). All scale bars (down left side) are 0.5 μm long.

Figure 3.

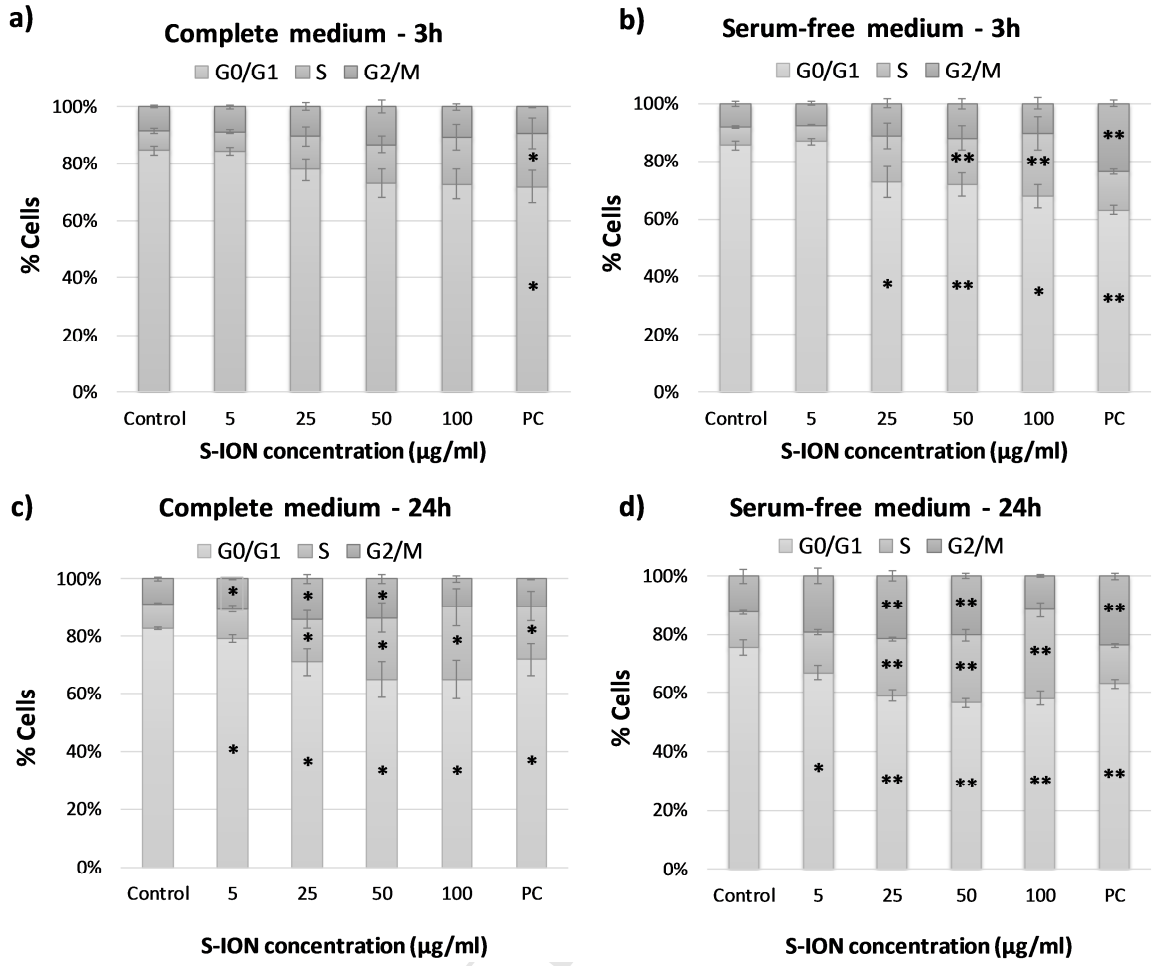

Fig. 3. Analysis of A172 cell cycle after treatment with S-ION for 3 h in complete medium (a) and serum-free medium (b), or for 24 h in complete medium (c) and serum-free medium (d). Bars represent mean ± standard error. PC: positive control (1.5 µM MMC). **P*<0.05, ***P*<0.01, significant differences with regard to the corresponding negative control.

Figure 4.

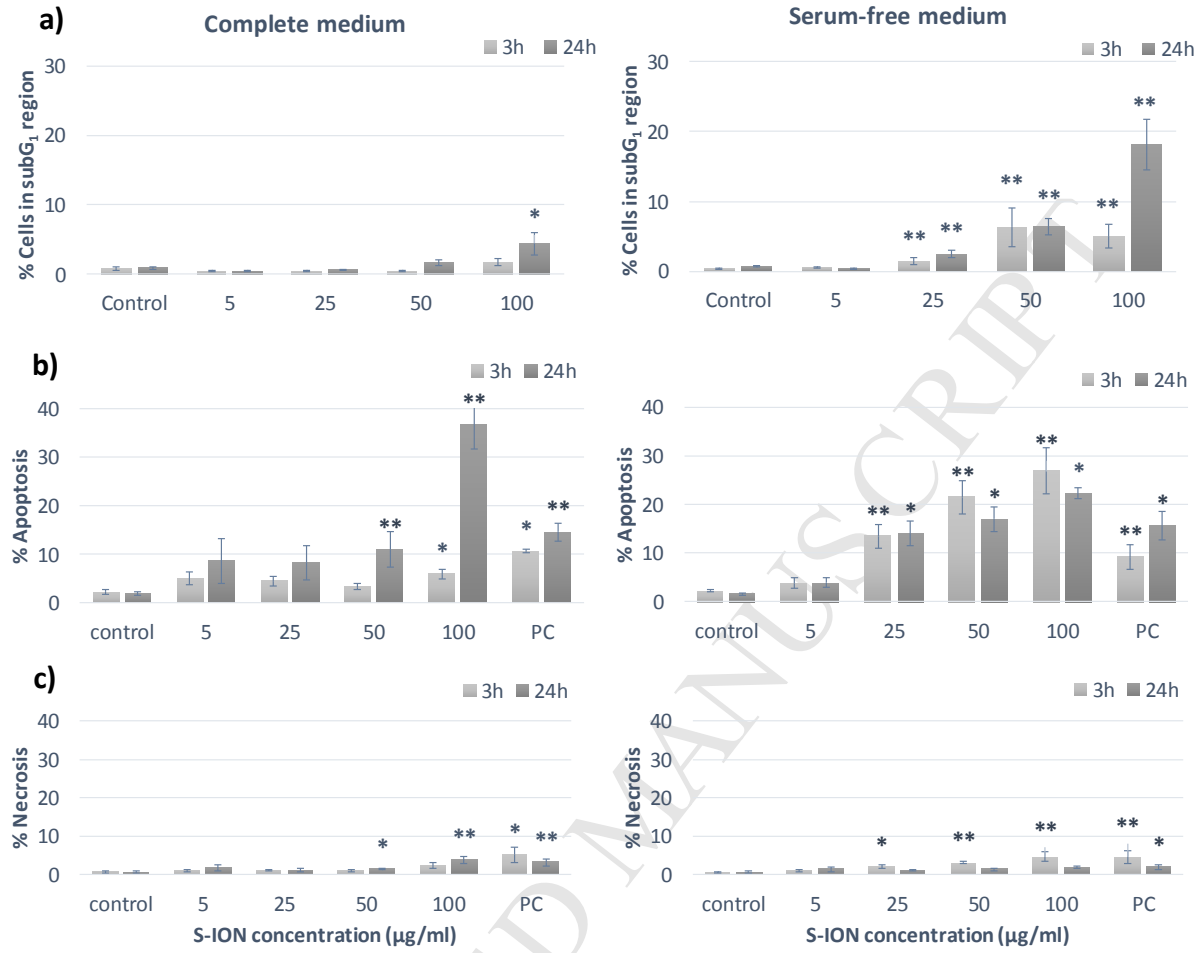

Fig. 4. Cell death induction by exposure of A172 cells to S-ION for 3 and 24 h in complete (left) and serum-free (right) medium. (a) Cells in the subG1 region of cell cycle distribution; (b) apoptosis rate and (c) necrosis rate, according to annexin V/propidium iodide double staining. Bars represent the mean ± standard error. PC: positive control (10 µM Campt). **P*<0.05, ***P*<0.01, significant difference with regard to the negative control.

Figure 5.

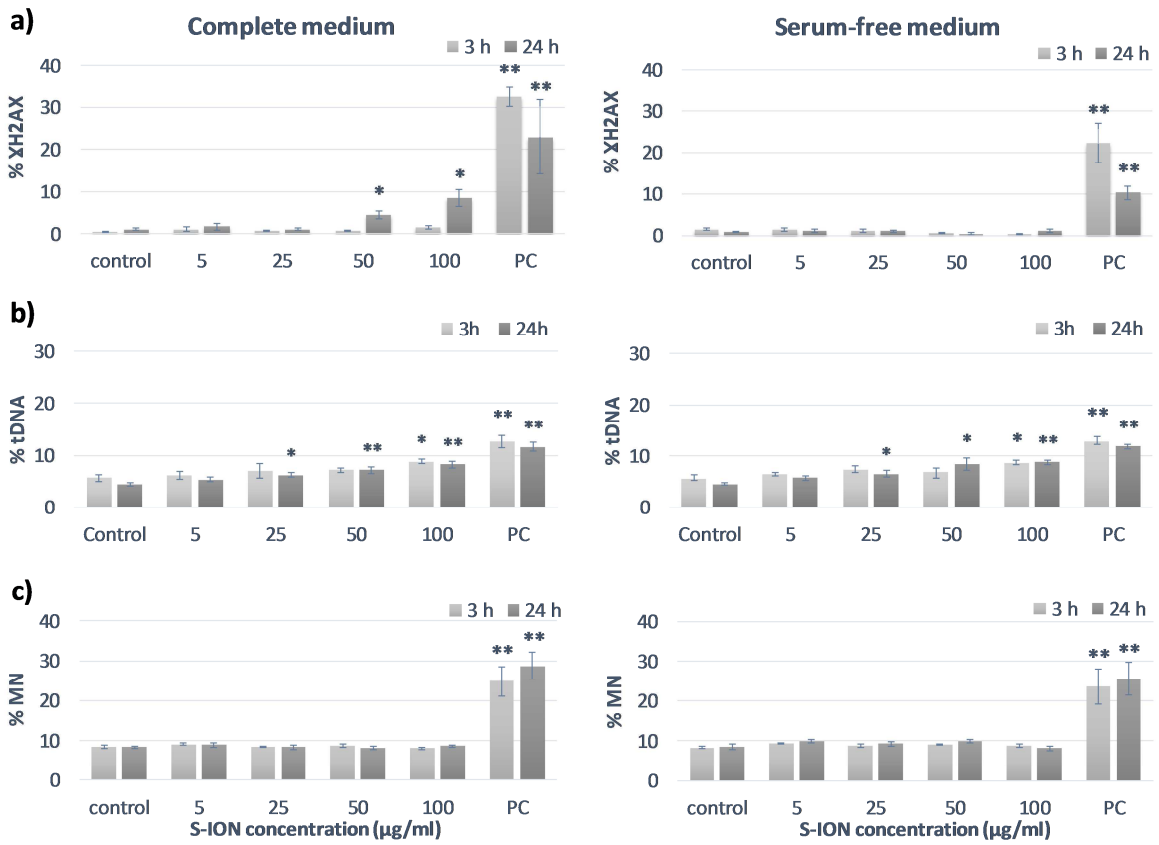

Fig. 5. Genotoxicity assessment of glial cells after treatment with S-ION dispersed in complete (left) and serum-free (right) medium. (a) H2AX histone phosphorylation, PC: positive control (1 µg/ml BLM); (b) primary DNA damage, as evaluated by the comet assay, PC: positive control (100 µM H2O2); and (c) micronuclei rates, PC: positive control (15 µM MMC). Bars represent mean ± standard error. *P<0.05, **P<0.01, significantly different from the negative control.

Figure 6.

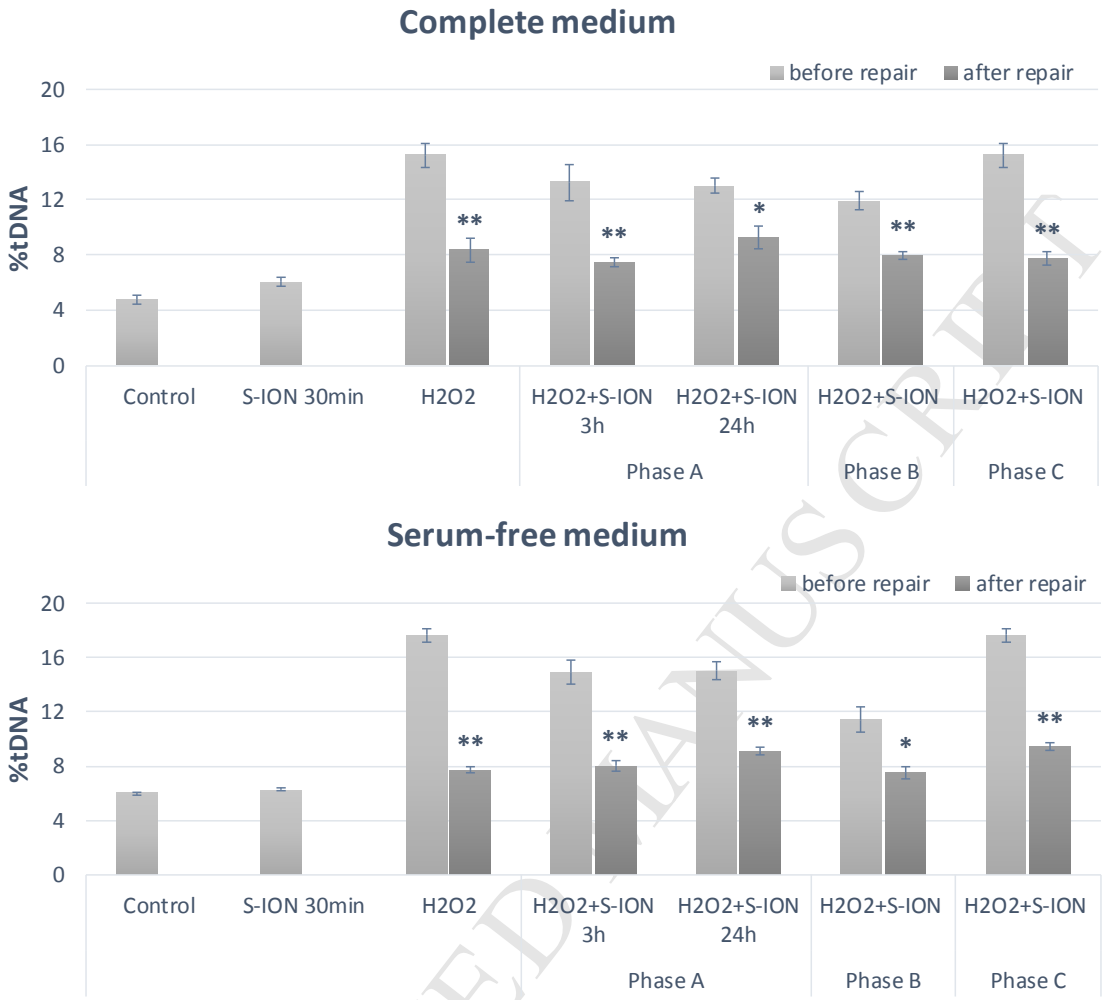

Fig. 6. Effects of S-ION on repair of H_2O_2-induced DNA damage in astrocytes in complete and serum-free medium. Incubation with S-ION was performed independently prior to exposure to 200 µM H_2O_2 (phase A, for 3 or 24 h), simultaneously with H_2O_2 (phase B), or during the repair period (phase C). Bars represent mean ± standard error. **P*<0.05, ***P*<0.01, significant difference with regard to the same treatment before repair.

Graphical Abstract

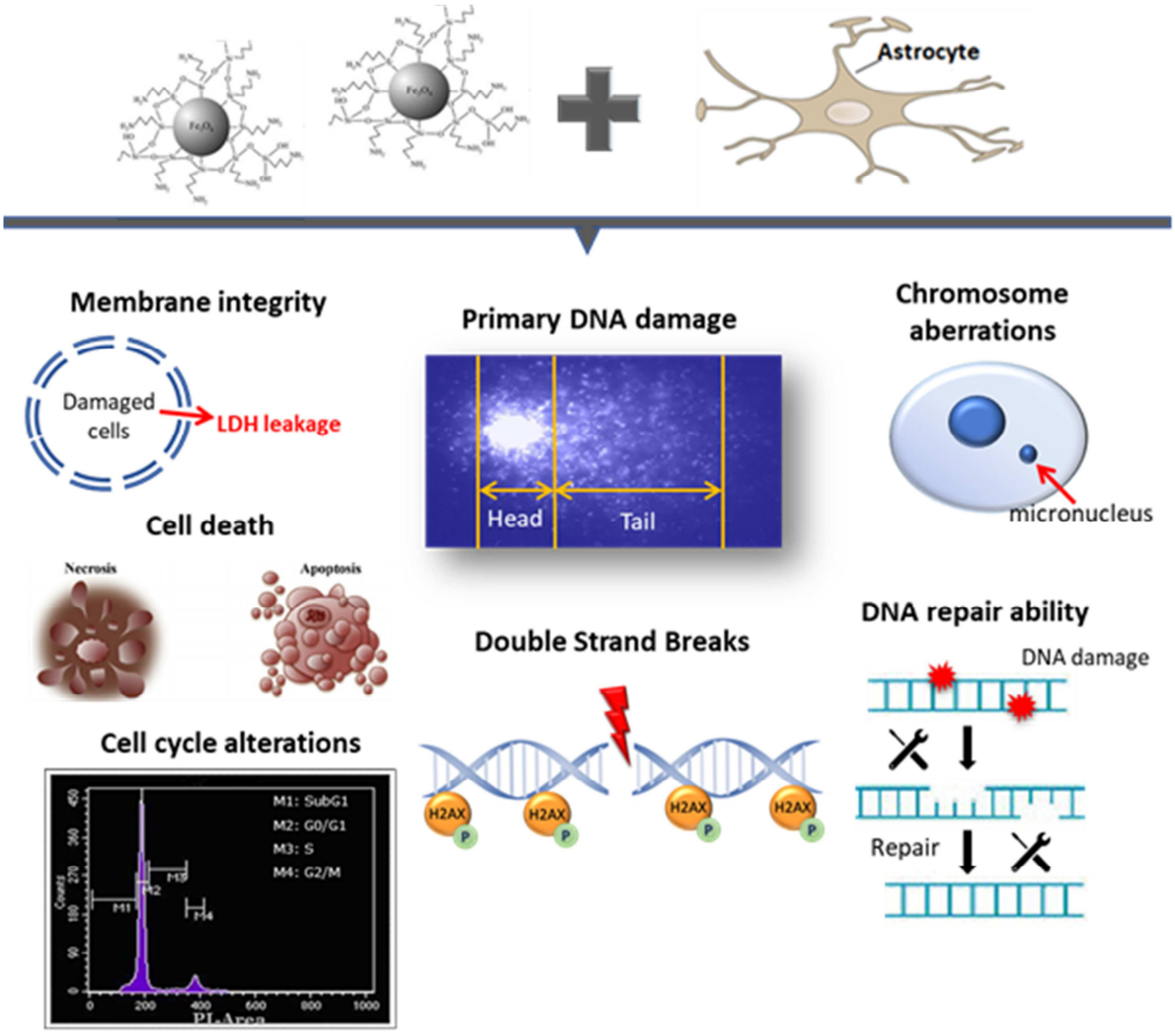

Highlights

- Iron oxide nanoparticles (ION) have great potential for different biomedical uses
- Knowing ION effects on nervous system is imperative, but studies are still scarce
- Cyto- and genotoxicity of silica-coated ION was evaluated on human A172 cells
- ION showed certain cytotoxicity, related to cell cycle disruption and cell death
- Scarce genotoxic effects and no alteration of the DNA repair process were observed